THE JOURNAL OF BIOLOGICAL CHEMISTRY
Vol. 273, No. 15, Issue of April 10, pp. 8572–8580, 1998

Printed in U.S.A.

In Vitro Cleavage of Internally Quenched Fluorogenic Human Proparathyroid Hormone and Proparathyroid-related Peptide Substrates by Furin

GENERATION OF A POTENT INHIBITOR*

(Received for publication, August 21, 1997, and in revised form, January 7, 1998)

Claude Lazure‡, Dany Gauthier‡, Francois Jean‡, Alain Boudreault‡, Nabil G. Seidah§, Hugh P. J. Bennett¶‖, and Geoffrey N. Hendy¶‡‡§§**

*From the ‡Laboratory of Neuropeptide Structure and Metabolism and the §J. A. DeSève Laboratory of Biochemical Neuroendocrinology, Institut de Recherches Cliniques de Montreal (Affiliated with the University of Montreal), Montreal, Quebec H2W 1R7 and the Departments of ¶Medicine, **Physiology, and ‡‡Human Genetics, McGill University and Royal Victoria Hospital, Montreal, Quebec H3A 1A1, Canada*

The cleavage of parathyroid hormone (PTH) from its precursor proparathyroid hormone (pro-PTH) is accomplished efficiently by the proprotein convertase furin (Hendy, G. N., Bennett, H. P. J., Gibbs, B. F., Lazure, C., Day, R., and Seidah, N. G. (1995) *J. Biol. Chem.* 270, 9517–9525). We also showed that a synthetic peptide comprising the −6 to +7 sequence of human pro-PTH is appropriately cleaved by purified furin *in vitro*. The human pro-PTH processing site Lys-Ser-Val-Lys-Lys-Arg differs from the consensus furin site Arg-Xaa-(Lys/Arg)-Arg that is represented by Arg-Arg-Leu-Lys-Arg in the cleavage site of pro-PTH-related peptide (pro-PTHrP). An earlier study demonstrated that an internally quenched fluorogenic substrate bearing an *O*-aminobenzoyl fluorescent donor at the NH_2 terminus and an acceptor 3-nitrotyrosine near the COOH terminus was appropriately cleaved by the convertases furin and PC1 (Jean, F., Basak, A., DiMaio, J., Seidah, N. G., and Lazure, C. (1995) *Biochem. J.* 307, 689–695). Here, we have synthesized a series of internally quenched fluorogenic substrates based upon the pro-PTH and pro-PTHrP sequences to determine which residues are important for furin cleavage. Purified recombinant furin and PC1 cleaved the human pro-PTH internally quenched substrate at the appropriate site in an identical manner to that observed with the nonfluorescent peptide. Several substitutions in the P_6–P_3 sequence were well tolerated; however, replacement of the Lys at the P_6 position with Gly and replacement of the P_3 Lys by an acidic residue led to markedly compromised cleavage by furin. Furin activity was very sensitive to substitution in P′ positions. Replacement of Ser at P_1' with Gly and Val at P_2' with Ala generated substrates that were less well cleaved. Substitution at the P_1' position of Val for Ser in conjunction with Ala for Val at P_2', as well as a single substitution of Lys for Val at P_2', generated specific inhibitors of furin cleavage. The findings of this study open the way to the rational design of inhibitors of furin with therapeutic potential.

Polypeptide hormones, such as parathyroid hormone (PTH)[1] which is the major regulator of extracellular calcium homeostasis (1) and many other biologically active proteins and peptides, including PTH-related peptide (PTHrP), are initially synthesized as larger inactive precursor proteins that undergo processing to release the active moiety. The related PTH gene family member, PTHrP, was originally recognized as the major pathogenic agent in the hypercalcemia of malignancy syndrome (2). Under normal physiological conditions it subserves a variety of autocrine or paracrine roles such as modulator of the growth of various cell types including cartilage, bone, skin, and breast, or regulator of vascular smooth muscle tone (3). Among the proprotein precursors, pro-PTH is unusual in that the excised pro-segment consists of only a hexapeptide (4) located NH_2-terminal to the 84-amino acid bioactive hormone. Pro-PTHrP is very similar to pro-PTH at the NH_2 terminus (5) with a predicted pro-segment of 12 amino acids (6).[2] In contrast to pro-PTH which is expressed almost exclusively in the parathyroid gland, pro-PTHrP is widely expressed in both nonendocrine and neuroendocrine cells.

Several mammalian subtilisin-like serine endoproteases having distinct or overlapping cleavage specificities have been identified that process proteins by cleaving carboxyl-terminally to pairs of basic residues and sometimes single basic residues (for review see Refs. 7–11). The most well characterized members of this enzyme family are furin, which is expressed in all cells, has a neutral pH optimum, contains a transmembrane region, and functions in the *trans*-Golgi network, and PC1 and PC2, which are localized exclusively to neuroendocrine cells, have more acidic pH optima, and act predominantly within secretory granules. In the parathyroid chief cell, pro-PTH is cleaved to PTH in the *trans*-Golgi network (12) rather than in secretory granules. This is consistent with processing of pro-PTH by furin or a furin-like enzyme rather than PC1 or PC2. Our previous studies demonstrated that when human (h) pre-pro-PTH (13) was coexpressed with the various members of the proprotein convertase family known at that time, in either a constitutively secreting cell line or a neuroendocrine cell line

* This work was supported in part by Medical Research Council of Canada Grants MT-9315, MT-6733, and PG-11474. The costs of publication of this article were defrayed in part by the payment of page charges. This article must therefore be hereby marked "*advertisement*" in accordance with 18 U.S.C. Section 1734 solely to indicate this fact.

‖ To whom correspondence should be addressed: Endocrine Laboratory, Rm. L2.05, Royal Victoria Hospital, 687 Pine Ave. West, Montreal, Quebec H3A 1A1, Canada. Tel.: 514-842-1231 (ext. 6731); Fax: 514-843-1709; E-mail: bennett@pathology.lan.mcgill.ca.

§§ Scientist of the Medical Research Council of Canada.

[1] The abbreviations used are: PTH, parathyroid hormone; pro-PTH, proparathyroid hormone; PTHrP, parathyroid hormone-related peptide; pro-PTHrP, proparathyroid hormone-related peptide; RP, reversed-phase; HPLC, high performance liquid chromatography; CF_3COOH, trifluoroacetic acid; MCA, 4-methylcoumaryl-1-amide; Abz, *o*-aminobenzoyl; Tyr(3-No_2), 3-nitrotyrosine; QFS, quenched fluorescent substrate; Boc, *t*-butoxycarbonyl; Fmoc, *N*-(9-fluorenyl)methoxycarbonyl; <Glu, pyroglutamic acid.

[2] G. N. Hendy, unpublished observations.

bearing a regulated secretory pathway, the most efficient processing was obtained with furin (14). Additionally, whereas furin is expressed in the parathyroid cell, PC1 and PC2 are not (14, 15).

In the vast majority of proproteins cleaved by furin, the processing site is of the consensus Arg-Xaa-(Arg/Lys)-Arg (P_4–P_1)[3] (17–19). However, in some cases, a sequence with two out of three basic residues at P_6, P_4, or P_2, in addition to the P_1Arg, or even Arg-Xaa-Xaa-Arg can constitute a competent furin site (20, 21). The human pro-PTH processing site Lys-Ser-Val-Lys-Lys-Arg (P_6–P_1) corresponds to one of the less commonly found sites, whereas the pro-PTHrP processing site Arg-Arg-Leu-Lys-Arg (P_5–P_1) conforms to the typical furin site, and its processing to PTHrP is thought to be mediated by this proprotein convertase (22). We have shown previously that a synthetic tridecapeptide corresponding to the −6 to +7 sequence of human pro-PTH was efficiently cleaved at the appropriate site carboxyl-terminal to the -(P_2)Lys-(P_1)Arg sequence by purified furin *in vitro* (14). Furthermore, we showed that an internally quenched fluorogenic substrate incorporating the proprotein cleavage site of the PC1 enzyme was a useful substrate to study convertase enzymatic activity (23). In the present study we synthesized an internally quenched fluorogenic substrate based upon the pro-PTH (−6 to +7) sequence bearing an *O*-aminobenzoyl fluorescent donor at the amino terminus and quenching 3-nitrotyrosine acceptor toward the carboxyl terminus. Having established this was appropriately cleaved by furin, we synthesized a series of similar substrates based upon the furin processing sites of both pro-PTH and pro-PTHrP to determine which residues are important for furin activity.

EXPERIMENTAL PROCEDURES

Materials—For fluorometric assays, the pentapeptide <Glu-Arg-Thr-Lys-Arg-MCA was obtained from Peptides International (Louisville, KY). The Fmoc-*O*-*N*-succinimide and the preloaded Fmoc-Ser-4-hydroxymethylphenoxy resin were purchased from Novabiochem (La Jolla, CA), and the Boc-anthranilic acid and (3-nitro)-Tyr were obtained from Bachem California (Torrance, CA) and Aldrich, respectively. The Fmoc-(3-nitro)-Tyr derivative was prepared as described (23), and its identity was confirmed by fast atom bombardment mass spectroscopy and ^{1}H NMR.

The endoprotease hfurin was obtained from conditioned medium of somatomammotroph GH_4C_1 cells infected with recombinant vaccinia virus bearing hfurin as described (14, 24) and was partially purified by anion exchange chromatography yielding a single immunoreactive band upon SDS-polyacrylamide gel electrophoresis and a single electrophoretic band after labeling with an octapeptidyl chloromethylketone inhibitor (24). Enzymatic activity was determined by a fluorometric assay using the substrate <Glu-Arg-Thr-Lys-Arg-MCA (24). Recombinant murine PC1 was obtained from the medium of Sf9 insect cells infected with baculovirus vector bearing murine PC1 and purified by ammonium sulfate precipitation.[4] This preparation contains two unique immunoreactive bands after SDS-PAGE which correspond to the full-length murine PC1 (87 kDa) and a COOH-terminal truncated form of 71 kDa both of which labeled with a pentapeptidyl chloromethylketone[4]. The enzymatic properties of this preparation are indistinguishable from our previously described partially purified virus produced murine PC1 (24). Enzymatically active murine PC2 was kindly provided by Dr. Iris Lindberg (Louisiana State University, New Orleans) and was purified from conditioned medium of Chinese hamster ovary PC2/7B2 expressing cells as described previously (25).

Design of Quenched Fluorescent Substrates—Our previous studies (14) showed that a peptide (human pro-PTH(−6 to + 7)) carboxyl-terminally extended relative to the cleavage site was cleaved more efficiently by furin than substrates comprising only the enzyme recognition site amino-terminal to the cleavage site. This implicated the importance of P′ positions in influencing enzyme activity. Therefore, the quenched fluorescent substrates were designed following our previous study (23) with the Abz donor group NH_2-terminal attached to position P_1, and the Tyr(3-NO_2) acceptor group was placed at P_5' sufficiently far from the cleavage site not to influence enzyme activity but not so far as to inordinately increase background fluorescence or reduce the intramolecular quenching effect (Fig. 1). A serine residue was placed at the carboxyl terminus to aid peptide solubility. Table I shows the 12 quenched fluorogenic substrates prepared which comprise the natural human pro-PTH (QFS-3) and rat pro-PTHrP (QFS-14) sequences, together with 10 substituted sequences which were designed to test the importance of positions P_6, P_5, P_4, P_3, P_1', and P_2' (QFS-4 to QFS-13).

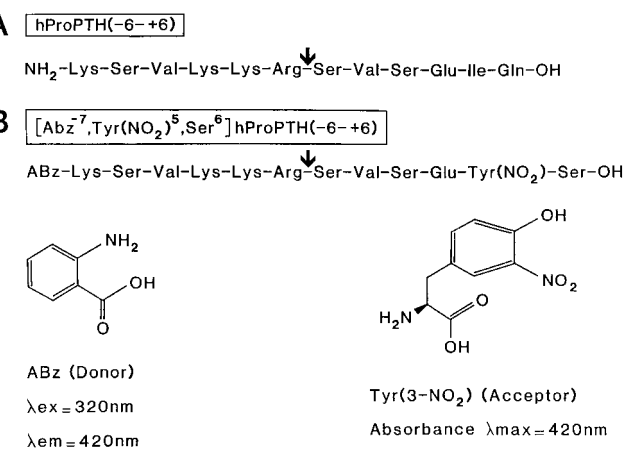

FIG. 1. *A*, amino acid sequence of human pro-PTH (−6 to +6). Site of cleavage is shown by the *arrow*. *B*, internally quenched fluorescent substrate based upon the human pro-PTH(−6 to +6) sequence. The highly fluorescent *o*-aminobenzoyl group is efficiently quenched by long range resonance energy transfer to the (3-nitro)-Tyr moiety.

Synthesis of Fluorescent and Other Peptidyl Substrates—All quenched fluorescent analogues (designated QFS-3 to QFS-14, see Table I), the fluorescent peptide, Abz-Lys-Ser-Val-Lys-Lys-Arg (designated FS-2), which represents the NH_2-terminal portion preceding the cleavage site in human pro-PTH, as well as a peptide (designated S-10) comprising Lys-Ser-Val-Lys-Lys-Arg-Ser-Lys-Ser-Glu-Tyr-Ser, which is the sequence of QFS-10 without the fluorescent and quencher moieties, were synthesized in the Peptide Synthesis Facility of the Sheldon Biotechnology Center, McGill University, using a symphony automated synthesizer (Rainin, Woburn, MA) according to previously described procedures (23). Following coupling of Fmoc-(3-nitro)-Tyr to preloaded H-Ser-4-hydroxymethylphenoxy resin, the peptide chain was elongated using Fmoc solid phase peptide chemistry until the final step when the Boc-anthranilic acid was added. The following side chain protecting groups were used: *t*-Boc for Lys, *t*-butyl for Ser and Asp, and 2,2,5,7,8-methylchroman-6-sulphonyl for Arg. Peptide derivatives were cleaved from the resin and deprotected by treatment with reagent K for 3 h (26), followed by lyophilization and repeated washing with ether.

Purification and Characterization of Fluorescent Substrates—The crude material from each synthesis was purified by reversed-phase high performance liquid chromatography (RP-HPLC), first using a semi-preparative CSC-Exsil C_{18} column (25 × 0.94 cm, Chromatography Sciences Co., St-Laurent, Quebec, Canada) and then an identical type of analytical column (25 × 0.46 cm). The buffer system comprised an aqueous 0.1% (v/v) CF_3COOH solution and an organic phase of acetonitrile containing 0.1% (v/v) CF_3COOH. Columns were eluted with a linear gradient from 5 to 60% organic phase in 60 min following a 5-min isocratic step at 5% organic phase; the flow rate was either 2.0 ml/min (semi-preparative) or 1.0 ml/min (analytical). The elution was monitored on-line by measurement of UV absorbance at 225 nm and the fluorescence at 420 nm after excitation at 320 nm in 1.0-ml fractions or on-line using a Varian Fluorichrom fluorescence detector. In the latter case, a combination of band filters (300–380 nm) was used for excitation of the fluorophor, whereas a sharp cut-off filter (>400 nm) was used in the emission window. Each purified peptide analogue was characterized by ion spray mass spectrometry using an AP1 111 triple stage mass spectrometer (Sciex, Thornhill, Ontario, Canada) as reported (14) and by amino acid analysis. Amino acid analyses were performed following 18–24 h hydrolysis in 5.7 N HCl at 110 °C *in vacuo* using a modified Beckman 120C autoanalyzer equipped with a Varian DS604 integrator/plotter.

Enzymatic Assays—Aqueous stock solutions (0.5–1.5 mM) of

[3] P_n nomenclature according to Schechter and Berger (16).

[4] A. Boudreault, N. G. Seidah, M. Chrétien, and C. Lazure, submitted for publication.

TABLE I
Quenched fluorogenic substrates

QFS no.	Amino acid sequence										Comments
	P_6	P_5	P_4	P_3	P_2	P_1	P_1'	P_2'	P_3'	P_4'[a]	
QFS-3	Abz[b]	K	S	V	K	K	R	S	V	S	Human Pro-PTH
QFS-4	Abz	K	S	V	**M**[c]	K	R	S	V	S	P_3 Met
QFS-5	Abz	**R**	S	V	**M**	K	R	S	V	S	P_6 Arg, P_3 Met
QFS-6	Abz	**G**	S	V	K	K	R	S	V	S	P_6 neutral
QFS-7	Abz	K	S	**R**	K	K	R	S	V	S	P_4 Arg
QFS-8	Abz	**G**	S	**R**	K	K	R	S	V	S	P_6 Gly, P_4 Arg
QFS-9	Abz	K	S	V	**E**	K	R	S	V	S	P_3 acidic
QFS-10	Abz	K	S	V	K	K	R	S	**K**	S	P_2' charged (basic)
QFS-11	Abz	K	S	V	K	K	R	S	**A**	S	P_2' neutral
QFS-12	Abz	K	S	V	K	K	R	**V**	**A**	S	P_1'-hydrophobic, P_2'neutral
QFS-13	Abz	K	S	V	K	K	R	**G**	V	S	P_1' Gly
QFS-14	Abz	**G**	**R**	**R**	**L**	K	R	**A**	V	S	Rat Pro-PTHrP

[a] Sequence positions are designated according to Schechter and Berger (16).
[b] Abz, *O*-aminobenzoyl (anthraniloyl); *Y*, 3-nitrotyrosine.
[c] Amino acids differing from those in the hPro-PTH sequence are in bold.

quenched fluorescence peptidyl substrates were stored at −20 °C. For enzymatic assay each substrate was incubated with the same amount of partially purified hfurin (4.9 μM/h AMC released, determined using the fluorogenic substrate <Glu-Arg-Thr-Lys-Arg-MCA) in 50 mM sodium acetate, pH 7.0, 1.0 mM $CaCl_2$ in a total volume of 100 μl. For murine PC1 the buffer used was 50 mM sodium acetate, pH 6.0, 10 mM $CaC1_2$, whereas for murine PC2, it was 50 mM sodium acetate, pH 5.5, 5 mM $CaCl_2$, and 0.1% Brij-30. Initial rate determinations were made in the presence of a range of peptidyl substrate concentrations (0.5–80 μM) at 25 °C in 96-well microtiter plates. Following addition of enzyme, the change in fluorescence was recorded with a Perkin-Elmer LS50B spectrofluorometer with a plate reader accessory using 320 and 420 nm as excitation and emission wavelength, respectively. The initial rate of cleavage (V_0) was determined with the built-in least square regression analysis system of the spectrofluorometer using the data recorded from 0 to 60 s after addition of the enzyme.

Correction for Quenching—The use of an extended sequence between the acceptor/donor pair can lead to significant background fluorescence as well as a decrease in the intramolecular quenching effect (23, 27). Although this can be problematic in stopped-time assays, it can be circumvented by coupling RP-HPLC analysis to each time point to measure directly the amount of product released. When multiple samples are to be analyzed, this method is tedious, and the use of initial velocity measurement with increasing concentrations of substrate is preferred. However, our initial results with this procedure showed that, in addition to a decrease in intramolecular quenching, there is a significant contribution from intermolecular quenching both between two substrate molecules with increasing concentration but also between a substrate molecule and the released fluorescent product. Whereas the former is not significant for substrate concentrations less than 40 μM, and the measured fluorescence is linear with respect to concentration of substrate (data not shown), the latter cannot be overlooked as the quenching appears rapidly. To correct for this, increasing amounts of the fluorescent NH_2-terminal cleavage product, FS-2, were incubated in the presence and absence of a single representative substrate (both QFS-2 and QFS-4 were used with similar results) at pH 6.0 and pH 7.0. The decrease in fluorescence concomitant upon the increase in substrate concentration up to 40 μM was thereby measured and used to correct the enzyme assay data. The change in fluorescence intensity per unit time was converted into μM/h values using a calibration curve based upon the fluorescence of FS-2 and correction of the quenching effect of increasing amounts of substrate on the fluorescence of the released product. For example, the equation slope = −0.064 [QFS-4] + 8.950 (correlation coefficient = 0.9555) was used to correct for quenching; the slope values were derived from the plot of the measured fluorescence of FS-2 *versus* [FS-2] in the presence of increasing amounts of QFS-4. Examples of the results are presented in the Appendix.

Determination of Kinetic Constants and Site of Cleavage—The kinetic parameters K_m and V_{max} were calculated with Enzfitter software version 1.03 (Elsevier Science Publishers, Amsterdam, The Netherlands). Data obtained over the 0.05–20 μM substrate range were fitted to the hyperbolic Michaelis-Menten rate equation. To determine the site of cleavage, at the end of the incubation period, reactions were stopped by the addition of excess EDTA, cleavage products separated by RP-HPLC, and their identities established by amino acid analysis.

Determination of Inhibitor Constants—The inhibitory characteristics of compounds QFS-10 and QFS-12 were investigated using stopped-time assays as well as initial rate assays as described above. Increasing amounts of peptide were mixed with a constant amount of hfurin in the presence of differing amounts of the fluorogenic substrate <Glu-Arg-Thr-Lys-Arg-MCA. Since these compounds could also quench the fluorescence produced by the released AMC, correction of the observed rate of cleavage was again required. Fluorescence quenching of AMC was linear up to 80 μM of QFS-12 and was corrected for by use of the equation slope = −0.004 [QFS-12] + 0.717 (correlation coefficient = 0.9703); the slope values were derived from the plot of the measured fluorescence of free AMC *versus* [AMC] in the presence of differing amounts of QFS-12. The two inhibitor constants (K_i and K_i') were determined by curve fitting of the data using Enzfitter software to Equation 1,

$$V_i/V_{max} = \frac{[S]/K_m}{1 + [S]/K_m + [I]/K_i + [I]/K_i' + [I]^2/K_iK_i' + 2[S][I]/K_mK_i} \quad \text{(Eq. 1)}$$

according to the inhibitor mechanism outlined in the Appendix. [S] and [I] denote the substrate and inhibitor concentration in μM, respectively, V_i and V_{max} the rate of cleavage in μM/h AMC released in the presence and in the absence of inhibitor, respectively, and K_m, K_i, and K_i' denote the rate constants.

The ability of peptide S-10 to inhibit cleavage of QFS-14 by hfurin was assessed. The K_i value was determined either by using Dixon's representation at three substrate concentrations (7.5, 10, and 15 μM) or by curve fitting of the data using the Enzfitter software to Equation 2.

$$V_i/V_{max} = \frac{[S]/K_m}{1 + [1]/K_i + [S]/K_m} \quad \text{(Eq. 2)}$$

In all cases, the velocity measurements were corrected for the quenching effect of increasing concentrations of QFS-14 on the release of the fluorescent product as described above.

RESULTS

Synthesis of the Quenched Fluorescent and Other Peptidyl Substrates—The observed amino acid compositions of all purified quenched fluorescent peptidyl substrates as well as the S-10 peptide were consistent with expected values (data not shown). For all substrates, with one exception, the observed molecular weights obtained by mass spectrometry were within 2 mass units of that expected (data not shown). In the case of QFS-5, although the amino acid composition was consistent with expected values, the molecular weight was some 96 mass units higher than expected. Given that a methionine residue is at position P_3, a likely explanation for the erroneous mass is that a side reaction yielding a trifluoroacetyl sulfonium salt occurred during final deprotection of the peptide.

Appropriate Cleavage of Quenched Fluorescent Peptidyl Substrates with Furin—All substrates were appropriately cleaved carboxyl-terminal to the (P_2)Lys-(P_1)Arg site. Fig. 2 shows a representative RP-HPLC chromatogram of the separation of digestion products of the substrate QFS-14 by hfurin. The substrate was cleaved at the expected site with production of

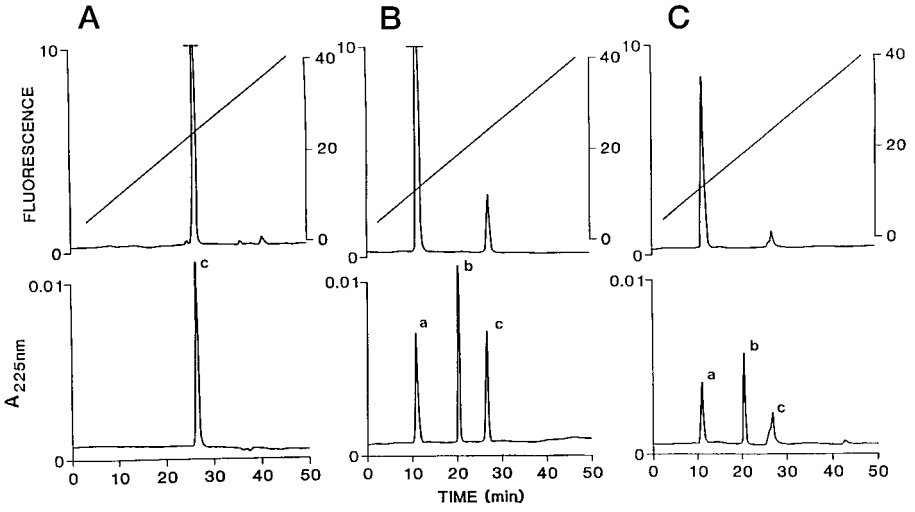

FIG. 2. **The pro-PTH quenched fluorescent substrates are appropriately cleaved at the correct site by furin.** Representative RP-HPLC chromatograms showing the separation of digestion products generated as described under "Experimental Procedures" of the internally quenched fluorogenic substrate QFS-14 by hfurin: *A*, 5.35 mmol of QFS-14, no enzyme; *B*, QFS-14, [S] = 60 μM, + furin; *C*, QFS-14, [S] = 15 μM, + furin. UV absorbance was monitored at 225 nm and fluorescence emission with a Fluorichrom on-line detector. The identity of peaks was made by amino acid analysis: *a*, NH_2-terminal fragment; *b*, COOH-terminal fragment; and *c*, undigested substrate.

the fluorescent NH_2-terminal fragment Abz-Gly-Arg-Arg-Leu-Lys-Arg and the nonfluorescent but UV-absorbing COOH-terminal fragment Ala-Val-Ser-Glu-(3-nitro)-Tyr-Ser.

The P′-elongated substrates are very efficiently cleaved, and this favors the use of initial velocity measurements for analysis of kinetic data. As shown in Fig. 3, more than 50% of the substrate (in this case 20 μM QFS-7) was cleaved by hfurin within 4 min. Upon much longer incubation times (90–1200 min) the presence of a guanidinoethyl mercaptosuccinic acid-inhibitable carboxypeptidase activity which removes the COOH-terminal basic residue from the NH_2-terminal fragment becomes apparent (Fig. 3, *inset*). The presence of a similar minor carboxypeptidase activity, as yet uncharacterized, was observed previously in recombinant vaccinia virus PC1 preparations (23).

Efficiency of Cleavage of Quenched Fluorescent Peptidyl Substrates with Furin—Representative plots of initial rate *versus* substrate concentration for substrates active with furin are shown in Fig. 4, and the kinetic constants corrected for substrate quenching are summarized for all substrates in Table II.

Substitutions at P Positions—For several of the substrates, substitutions in the P positions were well tolerated with relative V_{max}/K_m values ranging from 0.3 for the "typical furin site" of rat pro-PTHrP (QFS-14) to 1.0 for the human pro-PTH sequence itself (QFS-3) to 1.5 for an "optimized" human pro-PTH furin site (QFS-8) (see Table II). The sequence of the pro-PTH hexapeptide has been determined for several mammalian species (human, bovine, porcine, canine, rat, and mouse) and one avian (chicken) species. The choice of some of the QFS substitutions was guided by this knowledge. For example, although in mammalian species position P_3 is always occupied by Lys, in *avians* it is Met. Likewise, at position P_6 in all mammals Lys is present, and in avians Arg is substituted. Therefore, in QFS-4 Met substitutes for Lys at P_3, and in QFS-5, additionally, Arg substitutes for Lys at P_6. These substrates have V_{max} and relative V_{max}/K_m values not dissimilar to those of human pro-PTH (QFS-3) itself. Substitution of the P_4 Val with Arg, as in QFS-7, did not modify the kinetic parameters significantly, whereas additional substitution of the P_6 Lys with Gly, as in QFS-8, to generate a sequence conforming to the "classical" furin site led to a 2-fold increase in V_{max}.

One of the most deleterious substitutions was that of the P_6 Lys with Gly (QFS-6) emphasizing the critical role played by this residue in nonconsensus furin sites lacking a basic amino acid at P_4. Both an increase in K_m and decrease in V_{max} was noted with this substitution (Table II). Finally, whereas substitution of the P_3 Lys by a neutral amino acid (as in QFS-4) was well tolerated, furin cleavage was markedly compromised by substitution with Glu, an acidic amino acid. This was predominantly manifested by an increase in K_m.

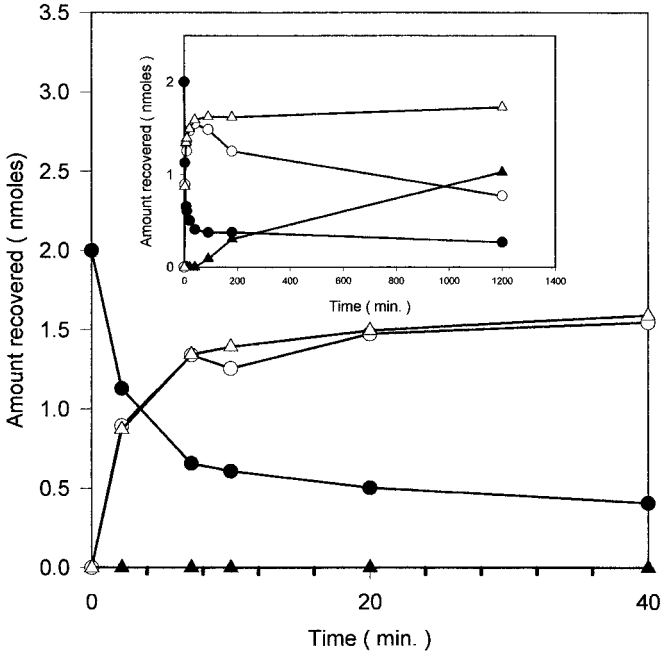

FIG. 3. **Time course analysis of the cleavage of QFS-7 by recombinant hfurin.** QFS-7 (20 μM) was incubated for increasing times with recombinant hfurin at pH 7.0. Aliquots were taken at each time point, and the products were analyzed by RP-HPLC as described under "Experimental Procedures" and as shown in Fig. 2. The main figure depicts the analysis up to 40 min, and the *inset* shows an extended analysis up to 20 h. QFS-7, Abz-Lys-Ser-Arg-Lys-Lys-Arg-Ser-Val-Ser-Glu-(NO_2)-Tyr-Ser (●); the complete NH_2-terminal fragment, Abz-Lys-Ser-Arg-Lys-Lys-Arg (○); which, upon longer incubation times (*inset*) is transformed by an endogenous contaminating carboxypeptidase activity into its COOH-terminal truncated form, Abz-Lys-Ser-Arg-Lys-Lys (▲); COOH-terminal fragment, Ser-Val-Ser-Glu-(NO_2)-Tyr-Ser (△).

Substitutions in P′ Positions—Examination of compilations of furin sites (29–31) in proproteins reveals that P_1' is often, although not always, a Ser residue as in human pro-PTH, and P_2' is an aliphatic hydrophobic residue such as Val. We found that furin activity is very sensitive to substitution in P′ positions. Substitution of P_2' which is Val in both human pro-PTH (QFS-3) and rat pro-PTHrP (QFS-14) with Lys yielded a compound (QFS-10) that was not cleaved. Likewise, substitution of Val at P_1' in conjunction with Ala at P_2' again led to a non-

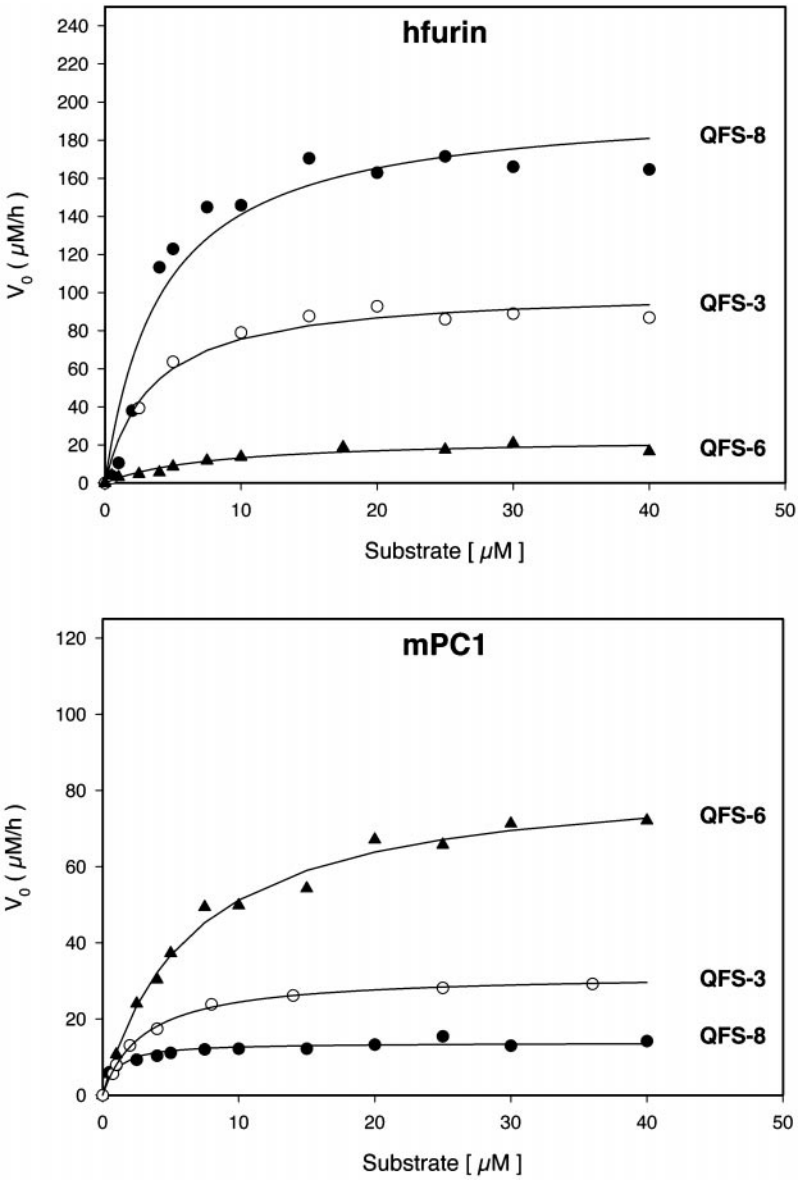

FIG. 4. **Representative plots of the initial rate of cleavage (V_0) *versus* substrate concentration, [S], for selected substrates, QFS-3, QFS-6, and QFS-8, obtained with hfurin (*top panel*) and murine PC1 (*bottom panel*).** Enzyme assays and data analysis were carried out as described under "Experimental Procedures." Note the difference in the scale of the *y* axes of the hfurin and murine PC1 plots.

TABLE II
Kinetic constants for cleavage of internally quenched fluorescent pro-PTH substrates with hfurin

Substrate	Sequence	K_m	V_{max}	V_{max}/K_m	V_{max}/K_m relative	k_{cat}/K_m	$\Delta(\Delta G)^b$
		μM	$\mu M/h$	h^{-1}		$M^{-1}\ s^{-1} \times 10^3$	$kcal/M$
QFS-3	Abz-KSVKKR-SVSEYS	4.6 ± 0.7[a]	115 ± 6[a]	25.19	**1.00**	199.9	
QFS-4	Abz-KSV**M**KR-SVSEYS	20 ± 1.2	113 ± 5	5.76	0.22	45.7	+0.875
QFS-5	Abz-**R**SV**M**KR-SVSEYS	20 ± 7	157 ± 38	7.88	0.31	62.6	+0.689
QFS-6	Abz-**G**SVKKR-SVSEYS	17 ± 5	37 ± 7	2.17	0.09	17.2	+1.455
QFS-7	Abz-KS**R**KKR-SVSEYS	5 ± 1.5	138 ± 17	25.70	1.02	204.1	−0.012
QFS-8	Abz-GS**R**KKR-SVSEYS	7 ± 2.8	259 ± 50	37.65	1.49	298.9	−0.238
QFS-9	Abz-KSV**E**KR-SVSEYS	37 ± 22	53 ± 23	1.42	0.06	11.3	+1.703
QFS-10	Abz-KSVKKR-S**K**SEYS	NC[c]	NC[c]			NC[c]	NC[c]
QFS-11	Abz-KSVKKR-S**A**SEYS	5.5 ± 1.2	35 ± 3	6.29	0.25	49.9	+0.822
QFS-12	Abz-KSVKKR-**VA**SEYS	NC[c]	NC[c]			NC[c]	NC[c]
QFS-13	Abz-KSVKKR-**G**VSEYS	9.2 ± 0.3	2.8 ± 0.1	3.02	0.11	23.9	+1.259
QFS-14	Abz-**GRR**LKR-**A**VSEYS	9 ± 4	59 ± 13	6.70	0.26	53.2	+0.785

[a] Mean ± S.D. (n = 3).
[b] This value was computed according to the equation $\Delta(\Delta G) = RT \times \ln[(k_{cat}/K_m)_A/(k_{cat}/K_m)_B]$ (28) where the subscripts A and B correspond to the reference compound (QFS-3) and the one of interest, respectively.
[c] Indicates that the substrate is not cleaved and behaves as an inhibitor when the activity is assayed with <ERTKR-MCA.

cleaved compound (QFS-12). Replacement of Val at P_2' with Ala yielded a substrate (QFS-11) that was cleaved but with a reduced V_{max}, and substitution of P_1' with Gly generated a substrate (QFS-13) with a V_{max} that was reduced still further.

Efficiency of Cleavage of Quenched Fluorescent Peptidyl Substrates with PC1—Representative plots of initial rate *versus* substrate concentration with murine PC1 are shown in Fig. 4, and for all substrates the kinetic constants corrected for sub-

TABLE III
Kinetic constants for cleavage of internally quenched fluorescent pro-PTH substrates with mPCI

Substrate	Sequence	K_m	V_{max}	V_{max}/K_m	V_{max}/K_m relative
		μM	$\mu M/h$	h^{-1}	
QFS-3	Abz-KSVKKR-SVSEYS	3.1 ± 0.2	31.9 ± 0.6	10.4	0.55
QFS-4	Abz-KSV**M**KR-SVSEYS	1.7 ± 0.5	11.6 ± 0.8	6.9	0.36
QFS-5	Abz-**R**SV**M**KR-SVSEYS	2.3 ± 0.6	16 ± 1	7.0	0.37
QFS-6	Abz-**G**SVKKR-SVSEYS	6.8 ± 1	86 ± 5	12.75	0.67
QFS-7	Abz-KS**R**KKR-SVSEYS	0.75 ± 0.2	7.7 ± 0.4	10.1	0.53
QFS-8	Abz-GS**R**KKR-SVSEYS	0.7 ± 0.1	12.8 ± 0.3	19.0	**1.00**
QFS-9	Abz-KSV**E**KR-SVSEYS	1.4 ± 0.2	9.8 ± 0.4	6.9	0.36
QFS-10	Abz-KSVKKR-S**K**SEYS	16 ± 4	23 ± 3	1.4	0.07
QFS-11	Abz-KSVKKR-SA**S**EYS	2.7 ± 0.3	32 ± 1	11.7	0.67
QFS-12	Abz-KSVKKR-**VA**SEYS	14 ± 6	5 ± 1	0.4	0.02
QFS-13	Abz-KSVKKR-**G**VSEYS	4.6 ± 0.4	36 ± 1	7.7	0.40
QFS-14	Abz-**GRRL**KR-**A**VSEYS	3.3 ± 0.9	18 ± 2	5.6	0.29

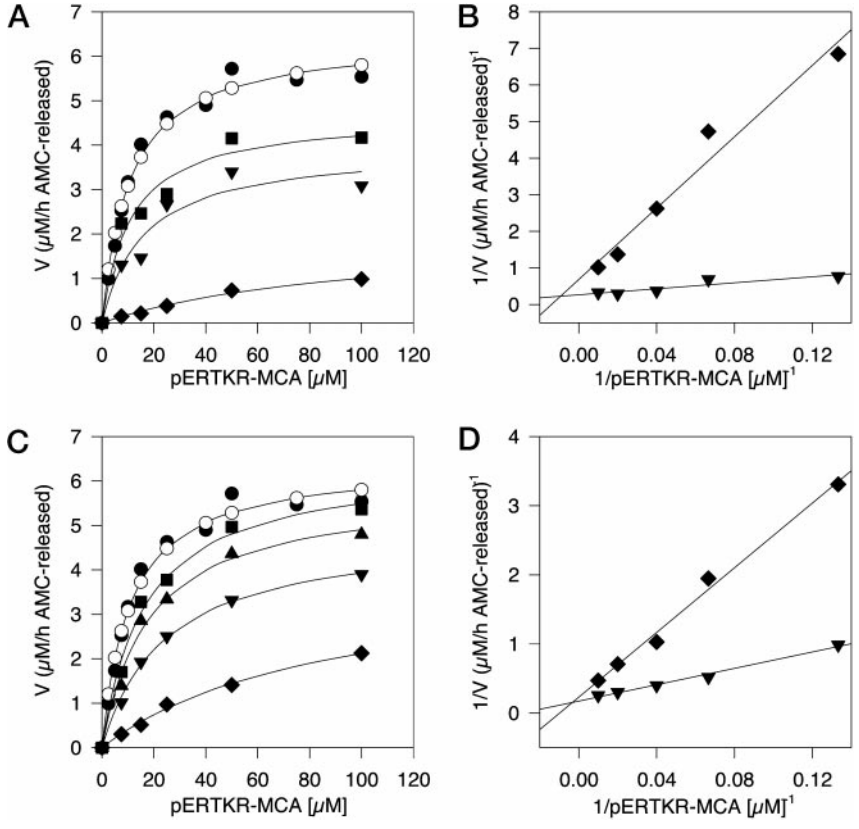

FIG. 5. **Inhibition of hfurin cleavage of <Glu-Arg-Thr-Lys-Arg-MCA by QFS-10 and QFS-12.** The rate of release of AMC from the fluorogenic substrate <Glu-Arg-Thr-Lys-Arg-MCA by the action of furin was measured in the absence (●) or the presence of the following concentrations of QFS-10 (*A*) or QFS-12 (*C*): 10 μM (■), 15 μM (▲), 25 μM (▼), and 50 μM (♦). The data points represent the values corrected for AMC fluorescence quenching, and the curves are the best fit hyperbolae. The computed data points from the best fit hyperbolae in the absence of inhibitor are indicated by the *open circles*. Representative reciprocal plots using either 25 μM (▼) or 50 μM (♦) of QFS-10 (*B*) and QFS-12 are shown (*D*).

strate quenching are summarized in Table III. The best substrate for murine PC1, based upon the ratio V_{max}/K_m, was QFS-8 in which Gly substitutes for Lys at P_6 and Arg replaces Val at P_4 (Table III). However, all other substrates (including QFS-6 and QFS-9 that were not well cleaved by hfurin), with the exception of QFS-10 and QFS-12, were reasonably well cleaved by murine PC1. In the case of QFS-10, the poor cleavage was due to an increased K_m, whereas with QFS-12, both an increased K_m and a decreased V_{max} were noted (Table III).

QFS-10 and QFS-12 Are Inhibitors of Furin—As neither QFS-10 nor QFS-12 was cleaved by hfurin, we explored the possibility that they were inhibitors of furin. This was done by testing their ability to block hfurin activity on the <Glu-Arg-Thr-Lys-Arg-MCA fluorogenic substrate. The quenching of the AMC fluorescence in the presence of increasing concentrations of either compound was corrected as described for the QFS compounds. As shown in Fig. 5, both compounds inhibited the cleavage of the fluorogenic substrate by hfurin at low micromolar concentrations. Additionally, both compounds functioned as mixed type inhibitors as an increase in K_m values were concomitant with a decrease in observed V_{max} (32). This was confirmed by the reciprocal plot yielding straight lines intersecting the abscissa to the left of the 1/*V* axis. However, all replots, with the exception of the intercepts of the reciprocal plot *versus* [I], exhibited a strong parabolic character indicative of more than one molecule of inhibitor interacting with the enzyme (data not shown). From linear regression analysis of the intercept replots, $K_i' = 21.9 + 5.1$ μM (mean + S.D.) for QFS-10 and 43.5 + 1.0 μM for QFS-12. A K_i value could not be derived from this type of analysis due to the slope-parabolic nature of the slope replots. However, all kinetic constants could be derived from the equation in "Determination of Inhibitor Constants" under "Experimental Procedures" which was based upon the mechanism outlined in the Appendix. It can be deduced that the free enzyme (*E*) combines with the substrate (S) yielding the (*E*S) complex with $K_m = 6.4$ μM and $V_{max} = 10.9$ μM/h AMC released. However, the inhibitor (I) binds either *E*S to form a ternary complex I*E*S or an *E*I complex to bind another molecule of inhibitor generating a second type of ternary complex (I*E*I). The type of ternary complex formed will depend upon whether

TABLE IV
Inhibitor constants for QFS-10 and QFS-12 with hfurin

The K_i and K_i' values were determined using the curve fitting algorithm of the Enzfitter software from the equation described under "Experimental Procedures" based upon the proposed inhibition mechanism (see text).

Compound	[I]	K_i	K_i'
	μM	μM ± S.D.	μM ± S.D.
QFS-10	10.0	7.1 ± 3.8	15.1 ± 2.5
	15.0	4.5 ± 2.6	21.1 ± 5.9
	25.0	9.4 ± 5.5	28.5 ± 7.1
	50.0	2.0 ± 0.6	22.8 ± 5.0
	Mean value	5.7 ± 3.1	21.9 ± 5.1
QFS-12	10.0	4.4 ± 1.0	28.8 ± 4.1
	15.0	5.6 ± 1.3	34.3 ± 4.8
	25.0	5.9 ± 0.6	41.0 ± 2.6
	50.0	2.6 ± 0.4	57.9 ± 9.9
	Mean value	4.6 ± 0.8	41.0 ± 5.4

the first molecule of inhibitor binds within the active site (*E*I) or elsewhere (I*E*). Both compounds appear to interact in an identical fashion with the active site region as both K_i values are very similar being 5.7 and 4.6 μM for QFS-10 and QFS-12, respectively (see Table IV), and are also similar to the K_m values obtained with the various QFS-peptidyl substrates (Table II). On the other hand, there is a 2-fold difference in K_i' values for the two compounds, in agreement with the values obtained from linear regression analysis of the intercept replots, QFS-10 being the better of the two in binding to the alternate site.

The ability of the QFS-10 nonfluorescent peptide sequence (S-10) to inhibit cleavage of a pro-PTHrP substrate (QFS-14) by hfurin is illustrated in Fig. 6. The S-10 peptide behaves as a competitive inhibitor with a K_i of 5.5 ± 1.3 μM (derived from the Dixon plot) or 5.9 ± 0.3 μM (obtained from curve fitting using the equation for competitive inhibition described under "Experimental Procedures").

DISCUSSION

Chromogenic and fluorogenic substrates have been widely used in the study of proteolytic enzymes. Typically, the peptidyl portion of the enzyme recognition sequence is attached at the carboxyl terminus via the cleavage site to a chromophoric (*e.g.* 4-nitroaniline) or fluorophoric (*e.g.* aminomethylcoumarin) leaving group. The release of the chromophore which is monitored by increases in absorbance is an indicator of the enzyme activity. However, the presence of a bulky chromophoric group in the P_1' position often leads to suboptimal enzyme activity. In addition, these substrates lack amino acids on the P′ side of the scissile bond which may be critical for optimal enzyme activity. For these reasons a longer substrate which extends into the P′ positions is desirable (23, 33, 34). Although a nonfluorogenic peptide can be used, the derivation of kinetic parameters requires separation and quantitation of the cleavage products by RP-HPLC. This can become tedious when a series of peptidyl substrates is to be analyzed, and in this respect the quenched fluorescent substrate approach (23, 33) has distinct advantages.

We previously showed that both furin and PC1 can correctly cleave a tridecapeptide spanning the pro-PTH cleavage site (14, 24) but that furin was much more efficient (14). This has been confirmed in the present study with the equivalent pro-PTH quenched fluorescent substrate. The pro-PTHrP cleavage site (Arg-Arg-Leu-Lys-Arg (P_5–P_1)), which conforms to the typical furin site, has not been examined previously by the direct cleavage method. In this study, we demonstrated first that a pro-PTHrP-quenched fluorescent peptide substrate was appropriately cleaved at the bond carboxyl-terminal to Lys(P_2)-Arg(P_1). We then showed that, as with pro-PTH, furin was more efficient than PC1 in performing this cleavage. Unlike pro-PTH which is expressed almost exclusively in the endocrine cells of the parathyroid gland, pro-PTHrP is widely expressed in a variety of cell types of nonendocrine as well as neuroendocrine origin, and it might therefore be anticipated that the ubiquitously expressed furin or a related furin-like enzyme would be the convertase responsible for releasing PTHrP from pro-PTHrP rather than PC1 or PC2 which are expressed exclusively in endocrine and neuroendocrine cells. It has previously been shown that production of biologically active PTHrP can be inhibited by antisense furin RNA technology (22, 35), although it remains uncertain from those studies whether the processing of pro-PTHrP is due directly to furin or a different convertase which requires prior activation by furin. Importantly, we show here for the first time the direct action of furin in efficiently cleaving the pro-PTHrP substrate at the appropriate site. Introduction of antisense furin RNA into a hypercalcemia of malignancy associated tumor cell line led to a negative effect on tumor cell volume *in vivo* and positive effect on animal survival time (35). Thus development of potent inhibitors targeted to the furin site of pro-PTHrP may be of significant anti-neoplastic benefit. The studies described here point the way to the design of a new generation of inhibitors that will block pro-PTHrP cleavage.

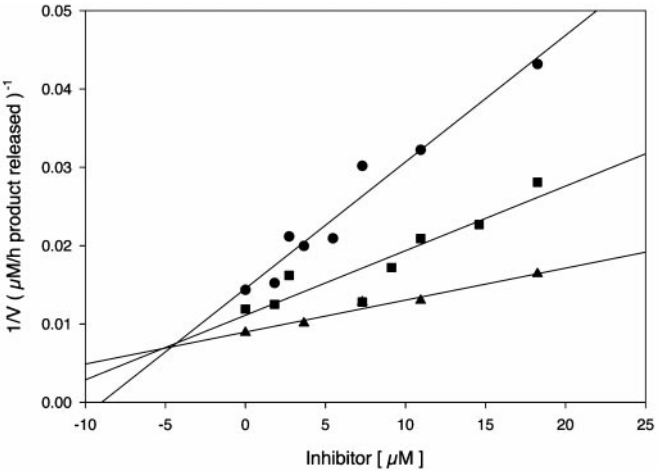

FIG. 6. **Inhibition of hfurin cleavage of QFS-14 by the nonfluorescent peptide Lys-Ser-Val-Lys-Lys-Arg-Ser-Lys-Ser-Glu-Tyr-Ser.** The rate of release of Abz-Gly-Arg-Arg-Leu-Lys-Arg from the quenched fluorescent substrate QFS-14 by the action of hfurin was measured in the presence of increasing amounts of inhibitor at three substrate concentrations: 7.5 μM (●), 10 μM (■), and 15 μM (▲). The data points represent the values after correction for quenching and peptide content. The *lines* were computed from linear regression analysis.

Previous studies have demonstrated the critical role played by the basic amino acids at positions P_2 and P_1 of the proprotein convertase recognition site. In the present study further insights were gained into what constitutes a competent furin site by focusing on changes at positions P_6-P_3, P_1', and P_2'. Several changes from the human pro-PTH sequence were well tolerated in the P_6–P_3 positions. However, furin cleavage was compromised by substitution of Glu for Lys at P_3 leading to a decreased affinity, whereas V_{max} remained unchanged. This may well be due to unfavorable interactions with the acidic residues postulated to form part of the binding pocket of furin which contacts the P_3 substrate residue (36–38). This could also explain for QFS-9 the large increase in relative transition state binding energy (Δ(Δ*G*) (28) of 1.7 kcal/mol resulting in a combined effect on recognition and cleavage. The P_6 Lys plays a critical role in nonconsensus furin sites such as that found in human pro-PTH which lack a basic amino acid at P_4. Substi-

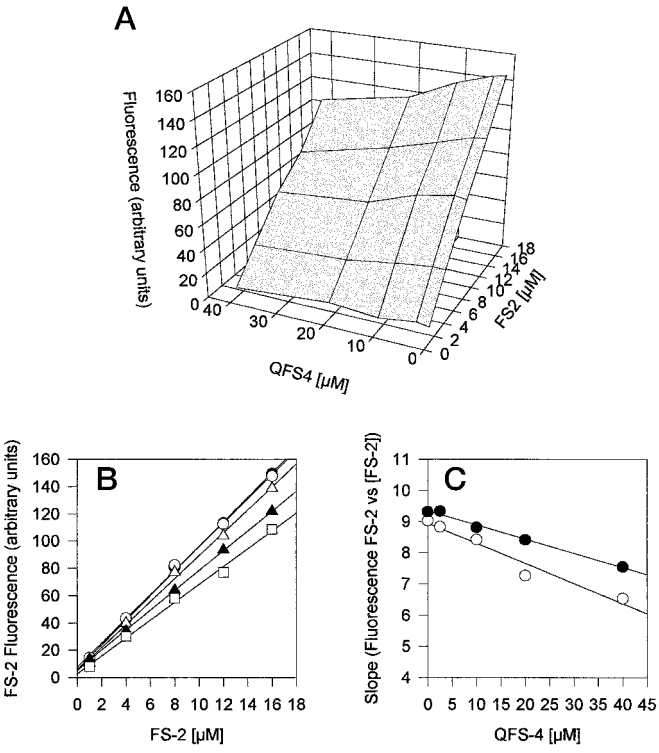

FIG. 7. **Fluorescence quenching of the cleaved product by increasing amounts of substrate.** *A*, three-dimensional representation of the effect of increasing concentrations of substrate (QFS-4) upon the fluorescence detected from increasing amounts of the product Abz-Lys-Ser-Val-Lys-Lys-Arg (FS-2). *B*, the fluorescence of increasing amounts of FS-2 was measured in the absence (●) or the presence of increasing amounts of QFS-4: 2.5 μM (○), 10 μM (△), 20 μM (▲), and 40 μM (□). *C*, changes in fluorescence as determined from the slopes of each line in *B* are plotted for pH 6.0 (●) and pH 7.0 (○) as a function of the concentration of QFS-4.

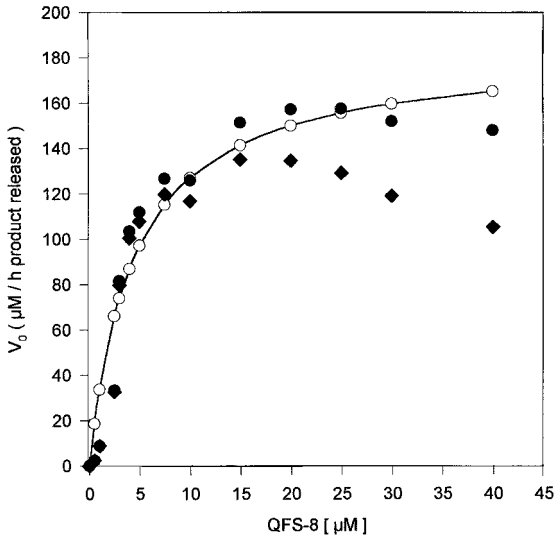

FIG. 8. **Representative graphical determination of the kinetic constants for QFS-8 and hfurin.** The rate of release of the NH_2-terminal fluorescent product by hfurin at pH 7.0 was measured by an on-line assay as described under "Experimental Procedures." The observed fluorescence was converted to μM/h units using a calibration curve based on the fluorescence of the FS-2 peptide as described in the text and shown in Fig. 7. ♦, raw data; ●, data corrected for the substrate quenching effect. Nonlinear regression analysis of the data from 0.5 to 20 μM QFS-8 for the best hyperbola yielded the curve (○) that was used for determination of the K_m and V_{max}.

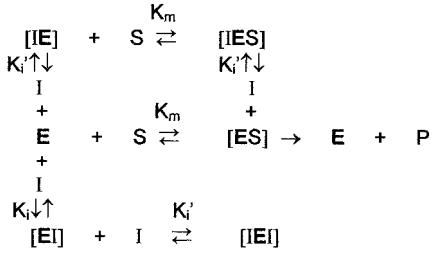

FIG. 9. **Schema of mixed type inhibition of enzyme activity.** The free enzyme (*E*) combines with the substrate yielding the (*E*S) complex. The inhibitor binds either (*E*S) to form a ternary complex (I*E*S) or an *E*I complex able to bind another molecule of inhibitor generating a second type of ternary complex (I*E*I). The type of ternary complex formed will depend upon whether the first molecule of inhibitor binds within the active site (*E*I) or elsewhere (*E*I). The equation describing this model that was used to compute K_i and K_i' is under "Experimental Procedures."

tution of Gly for Lys at position P_6 reduced specificity for furin both by an increased K_m and V_{max}, whereas specificity for PC1 increased primarily through an altered V_{max}. This deleterious effect of removing the basic amino acid at P_6 could be compensated for by converting P_4 from Val to Arg thereby creating a consensus furin site.

Importantly, we show that furin and PC1 activities are very sensitive to certain substitutions in the P′ positions. This result was to be anticipated by previous studies showing poor cleavage of peptidyl substrates having non-natural and bulky residues at the P_1' position (39, 40) and those using small fluorogenic peptidyl-MCA substrates which indicated that the efficiency of cleavage depends more on the deacylation step than on the recognition step (21). For example, in the present studies, substitution of the P_1' Ser with Gly led to a substrate that was cleaved much less well, predominantly due to a reduced V_{max}. Strikingly, substitution of the P_1' Ser with Val in combination with replacement of the P_2' Val with Ala as well as the single substitution of the P_2'Val with Lys generated compounds that were not cleaved at all by furin and, additionally, were poorly cleaved by PC1. Interestingly, substitution in the proalbumin sequence of the P1′ Asp by Lys was found to completely abolish the removal of the propeptide by furin (20). Together with the present data, this implies that, for a proper furin cleavage, positions P1′ and P2′ should not be both occupied by a positively charged Lys residue or a hydrophobic aliphatic residue. In the present studies, further analysis established the inhibitory nature of the QFS-10 and QFS-12 compounds on furin activity. Both these compounds are specific inhibitors of furin, whereas they are cleaved by murine PC1 (Table III) at a rate of 9.5 and 1.6 μM/h, respectively, and QFS-10 is cleaved by murine PC2 at a rate of 0.81 μM/h when using a concentration of 20 μM. However, with furin these two substrates behave as mixed type competitive inhibitors (see Appendix, Fig. 9) and bind at two sites on the enzyme, one of which we hypothesize to be the substrate pocket itself and the other of unknown location.

This is the first example of (i) a peptidyl inhibitor that is apparently specific for furin, and (ii) an inhibitor for the proprotein convertases that binds at two sites on such enzymes. Concerning the first point, it should be noted that, for all the potential proprotein P_2' Lys-containing substrates, none appears to be a substrate for furin. The list of such proteins includes the pro-Müllerian inhibiting substance, proneurokinin A, propancreatic polypeptide, and proprotein tyrosine phosphatase-μ receptor. Both pro-Müllerian inhibiting substance and proprotein tyrosine phosphatase-μ receptor are cleaved by PC5 (41, 42), and propancreatic polypeptide is processed in the regulated secretory pathway by the neuroendocrine-specific enzymes, PC1 and PC2 (43). As far as the second point is

concerned, it is very unlikely that the substrate binding site would be able to accommodate two dodecapeptide inhibitor molecules simultaneously. Little is known about sites on convertases that bind other molecules as modulators of enzymatic activity with the exception of the neuroendocrine protein 7B2 and PC2 (44–46). This interaction is thought to involve the COOH-terminal inhibitory region of 7B2 acting within the active site of the enzyme and a second site comprising a proline-rich and α-helical region of the 7B2 molecule (47). We therefore propose that the sequence Arg-Xaa-(Lys/Arg)-Arg-Ser-Lys (P_4-P_2') could serve as the basis for designing further furin-specific inhibitors. We have already demonstrated in the present study that one such peptide, S-10, can inhibit furin cleavage of a pro-PTHrP substrate in a competitive fashion in the low micromolar range. In addition, in future studies it will be important to elucidate the nature of the secondary site targeted by some of these inhibitors. This will aid in improving inhibitor design even further.

Acknowledgments—We thank Susan James, Jing Hu, Bernard F. Gibbs, and Diane Savaria for their help with various aspects of this study. We also thank Dr. Marc Vaillancourt (IRCM) for helpful discussions and Debra Hamel and Pamela Kirk for preparation of the manuscript.

APPENDIX

Fluorescent Quenching of the Cleaved Product by Increasing Amounts of Substrate—To overcome the intermolecular quenching effect, varying amounts of the fluorescent NH_2-terminal cleavage product Abz-Lys-Ser-Val-Lys-Lys-Arg (FS-2) were incubated in the presence and absence of representative substrate; QFS-4 is shown in Fig. 7, but similar results were obtained with QFS-2 (data not shown). The linear decrease in fluorescence concomitant to the increase in substrate concentration up to 40 μM was measured and used to correct the raw fluorescence data obtained from the furin and PC1 enzyme assays.

Determination of Kinetic Constants for Quenched Fluorescent Substrates and Furin and PC1—Fig. 8 shows a representative graphical determination of the kinetic constants for QFS-8 and hfurin. The initial velocity data are presented and were obtained over a substrate range of 0.5 to 40 μM. The decrease in measured velocity due to increasing concentrations of substrate is evident at concentrations greater than 10 μM. Upon correction for intramolecular quenching, the curve is normalized toward the computed best fit curve. For substrates that are well cleaved, calculation of kinetic parameters from velocity measurements obtained at substrate concentrations lower than 10 μM gives values of V_{max}/K_m no different from those obtained after correction for intermolecular quenching or those obtained for selected substrates after stopped-time assays followed by RP-HPLC separation of products. However, the correction method was used throughout to derive the kinetic constants listed in Tables II and III.

Model of Mixed Type Competitive Inhibition—Fig. 9 presents a schema of mixed type inhibition of enzyme activity by the quenched fluorescent substrates that is compatible with the equation for V_i/V_{max} given under "Experimental Procedures."

REFERENCES

1. Hendy, G. N. (1997) in *Endocrinology: Basic and Clinical Principles* (Conn, P. M., and Melmed, S., eds) pp. 307–323, Humana Press Inc., Totowa, NJ
2. Halloran, B. P., and Nissenson, R. A. (eds) (1992) *Parathyroid Hormone-related Protein: Normal Physiology and Its Role in Cancer,* CRC Press, Boca Raton, FL
3. Moseley, J. M., and Martin, T. J. (1996) in *Principles of Bone Biology* (Bilezikian, J. P., Raisz, L. G., and Rodan, G. A., eds) pp. 363–376, Academic Press, San Diego
4. Hamilton, J. W., Niall, H. D., Jacobs, J. W., Keutmann, H. T., Potts, J. T., Jr., and Cohn, D. V. (1974) *Proc. Natl. Acad. Sci. U. S. A.* **71,** 653–656
5. Suva, L. J., Winslow, G. A. A., Wettenhall, R. E. H., Hammonds, R. G., Moseley, J. M., Diefenbach-Jagger, H., Rodda, C. P., Kemp, B. E., Rodriquez, H., Chen, E. Y., Hudson, P. J., Martin, T. J., and Wood, W. J. (1987) *Science* **237,** 893–895
6. Von Heijne, G. (1986) *Nucleic Acids Res.* **14,** 4683–4690
7. Seidah, N. G., Chrétien, M., and Day, R. (1994) *Biochimie* (*Paris*) **76,** 197–209
8. Steiner, D. F., Smeekens, S. P., Ohagi, S., and Chan, S. J. (1992) *J. Biol. Chem.* **267,** 23435–23438
9. Van De Ven, W. J. M., and Roebroek, A. (1993) *Crit. Rev. Oncog.* **4,** 115–136
10. Lindberg, I. (1991) *Mol. Endocrinol.* **5,** 1361–1365
11. Barr, P. J. (1991) *Cell* **66,** 1–3
12. Habener, J. F., Amherdt, M., Ravazzola, M., and Orci, L. (1979) *J. Cell Biol.* **80,** 715–731
13. Hendy, G. N., Kronenberg, H. M., Potts, J. T., Jr., and Rich, A. (1981) *Proc. Natl. Acad. Sci. U. S. A.* **78,** 7365–7369
14. Hendy, G. N., Bennett, H. P. J., Gibbs, B. F., Lazure, C., Day, R., and Seidah, N. G. (1995) *J. Biol. Chem.* **270,** 9517–9525
15. Scopsi, L., Gullo, M., Rilke, F., Martin, S., and Steiner, D. F. (1995) *J. Clin. Endocrinol. & Metab.* **80,** 294–301
16. Schechter, I., and Berger, B. (1967) *Biochem. Biophys. Res. Commun.* **27,** 157–162
17. Hosaka, M., Nagahama, M., Kim, W. S., Watanabe, T., Hatsuzawa, K., Ikemizu, J., Murakami, K., and Nakayama, K. (1991) *J. Biol. Chem.* **266,** 12127–12130
18. Watanabe, T., Murakami, K., and Nakayama, K. (1993) *FEBS Lett.* **320,** 215–218
19. Takahashi, S., Hatsuzawa, K., Watanabe, T., Murakami, K., and Nakayama, K. (1994) *J. Biochem.* (*Tokyo*) **116,** 47–52
20. Molloy, S. S., Bresnahan, P. A., Leppla, S. H., Klimpel, K. R., and Thomas, G. (1992) *J. Biol. Chem.* **267,** 16396–16402
21. Jean, F., Boudreault, A., Basak, A., Seidah, N. G., and Lazure, C. (1995) *J. Biol. Chem.* **270,** 19225–19231
22. Liu, B., Goltzman, D., and Rabbani, S. A. (1995) *Am. J. Physiol.* **268,** E832–E838
23. Jean, F., Basak, A., DiMaio, J., Seidah, N. G., and Lazure, C. (1995) *Biochem. J.* **307,** 689–695
24. Jean, F., Basak, A., Rondeau, N., Benjannet, S., Hendy, G. N., Seidah, N. G., Chrétien, M., and Lazure, C. (1993) *Biochem. J.* **292,** 891–900
25. Lamango, N. S., Zhu, X., and Lindberg, I. (1996) *Arch. Biochem. Biophys.* **330,** 238–250
26. King, D. S., Fields, C. G., and Fields, G. B. (1990) *Int. J. Pept. Protein Res.* **36,** 255–266
27. Meldal, M., and Breddam, K. (1991) *Anal. Biochem.* **195,** 141–147
28. Wilkinson, A. J., Fersht, A. R., Blow, D. M., and Winter, G. (1983) *Biochemistry* **22,** 3581–3586
29. Breshnahan, P. A., Hayflick, J. S., Molloy, S. S., and Thomas, G. (1993) in *Mechanisms of Intracellular Trafficking and Processing of Proproteins* (Loh, Y. P., ed) pp. 225–250, CRC Press, Boca Raton, FL
30. Seidah, N. G. (1995) in *Intramolecular Chaperones and Protein Folding* (Shinde, U., and Inoue, M., eds) pp. 181–203, R. G. Landes, Austin, TX
31. Denault, J. B., and Leduc, R. (1996) *FEBS Lett.* **379,** 113–116
32. Segel, I. H. (1993) *Enzyme Kinetics: Behavior and Analysis of Rapid Equilibrium and Steady-state Enzyme Systems*, pp. 161–226, John Wiley & Sons, Inc., New York
33. Angliker, H., Neumann, U., Molloy, S. S., and Thomas, G. (1995) *Anal. Biochem.* **224,** 409–412
34. Rockwell, N. C., Wang, G. T., Krafft, G. A., and Fuller, R. S. (1997) *Biochemistry* **36,** 1912–1917
35. Liu, B., Amizuka, N., Goltzman, D., and Rabbani, S. A. (1995) *Int. J. Cancer* **63,** 276–281
36. Roebroek, A. J. M., Creemers, J. W. M., Ayoubi, T. A. Y., and Van De Ven, W. J. M. (1994) *Biochimie* (*Paris*) **76,** 210–216
37. Siezen, R. J., Creemers, J. W. M., and Van De Ven, W. J. M. (1994) *Eur. J. Biochem.* **222,** 255–266
38. Siezen, R. J., and Leunissen, J. A. M. (1997) *Protein Sci.* **6,** 501–523
39. Basak, A., Jean, F., Seidah, N. G., and Lazure, C. (1994) *Int. J. Pept. Protein Res.* **44,** 253–261
40. Basak, A., Schmidt, C., Ismail, A. A., Seidah, N. G., Chrétien, M., and Lazure, C. (1995) *Int. J. Pept. Protein Res.* **46,** 228–237
41. Nachtigal, M. W., and Ingraham, H. A. (1996) *Proc. Natl. Acad. Sci. U. S. A.* **93,** 7711–7716
42. Campan, M., Yoshizumi, M., Seidah, N. G., Lee, M. E., Bianchi, C., and Haber, E. (1996) *Biochemistry* **35,** 3793–3802
43. Wulff, B. S., Johansen, T. E., Dalboge, H., O'Hare, M. M., and Schwartz, T. W. (1993) *J. Biol. Chem.* **268,** 13327–13335
44. Martens, G. J. M., Braks, J. A. M., Eib, D. W., Zhou, Y., and Lindberg, I. (1994) *Proc. Natl. Acad. Sci. U. S. A.* **91,** 5784–5787
45. Van Horssen, A. M., Van den Hurk, W. H., Bailyes, E. M., Hutton, J. C., Martens, G. J. M., and Lindberg, I. (1995) *J. Biol. Chem.* **270,** 14292–14296
46. Benjannet, S., Savaria, D., Chrétien, M., and Seidah, N. G. (1995) *J. Neurochem.* **64,** 2303–2311
47. Zhu, X., Lamango, N. S., and Lindberg, I. (1996) *J. Biol. Chem.* **271,** 23582–23587

In Vitro Cleavage of Internally Quenched Fluorogenic Human Proparathyroid Hormone and Proparathyroid-related Peptide Substrates by Furin: GENERATION OF A POTENT INHIBITOR

Claude Lazure, Dany Gauthier, Francois Jean, Alain Boudreault, Nabil G. Seidah, Hugh P. J. Bennett and Geoffrey N. Hendy

J. Biol. Chem. 1998, 273:8572-8580.
doi: 10.1074/jbc.273.15.8572